

δ -catenin promotes bevacizumab-induced glioma invasion

Toshihiko Shimizu, Joji Ishida, Kazuhiko Kurozumi, Tomotsugu Ichikawa, Yoshihiro Otani,
Tetsuo Oka, Yusuke Tomita, Yasuhiko Hattori, Atsuhito Uneda, Yuji Matsumoto, Isao Date

Department of Neurological Surgery, Okayama University Graduate School of Medicine,
Dentistry and Pharmaceutical Sciences, Okayama, Japan

Corresponding Author: Kazuhiko Kurozumi

Address: 2-5-1 Shikata-Cho, Kita-ku Okayama 700-8558, Japan,

Phone: +81-86-235-7336, Fax: +81-86-227-0191

E-mail: kkuro@md.okayama-u.ac.jp

Running title

Bevacizumab-induced glioma invasion

Financial Information

This study was supported by grants-in-aid for Scientific Research from the Japanese Ministry of Education, Culture, Sports, Science, and Technology to K. Kurozumi (No. 23592125; No. 26462182) & I. Date (No. 26670644).

Conflict of interest

None of the authors have any conflicts of interest to declare.

Keywords: glioma, invasion, bevacizumab, VEGF, δ -catenin

Abstract

The combination of bevacizumab with temozolomide and radiotherapy was shown to prolong progression-free survival in newly diagnosed glioblastoma patients, and this emphasizes the potential of bevacizumab as a glioma treatment. However, while bevacizumab effectively inhibits angiogenesis, it has also been reported to induce invasive proliferation. This study examined gene expression in glioma cells to investigate the mechanisms of bevacizumab-induced invasion. We made a human glioma U87 Δ EGFR cell xenograft model by stereotactically injecting these cells into the brain of animals. We administered bevacizumab intraperitoneally three times per week. At 18 days after tumor implantation, the brains were removed for histopathology and mRNA was extracted. *In vivo*, bevacizumab treatment increased glioma cell invasion. qRT-PCR array analysis revealed upregulation of δ -catenin (CTNND2) and several other factors. *In vitro*, bevacizumab treatment upregulated δ -catenin expression. A low concentration of bevacizumab was not cytotoxic, but tumor cell motility was increased in scratch wound assays and two-chamber assays. Overexpression of δ -catenin increased the tumor invasion *in vitro* and *in vivo*. On the other hand, δ -catenin knockdown decreased glioma cell invasiveness. The depth of tumor invasion in the U87 Δ EGFR cells expressing δ -catenin was significantly increased compared with empty vector-transfected cells. The increase in invasive capacity induced by bevacizumab therapy was associated with upregulation of δ -catenin expression in invasive tumor cells. This finding suggests that δ -catenin is related to tumor invasion and migration.

INTRODUCTION

Glioblastoma is the most destructive brain tumor. Despite the advances in basic and clinical research, glioblastoma patients have a poor prognosis, with a median survival time of around 14 months (1). Characteristics of malignant glioma include it being fast-growing, invasive, aggressive, and capable of angiogenesis. Recently, clinical trials to investigate drugs directed at molecular targets have been performed (2,3).

Vascular endothelial growth factor (VEGF), which promotes angiogenesis, is abundantly expressed by glioma cells. The results of trials with bevacizumab, an anti-VEGF antibody, showed significant effects for treatment of recurrent glioblastoma patients (4-6). The phase III AVAglia and RTOG 0825 studies indicated that the combination of bevacizumab, radiation, and temozolomide in newly diagnosed glioblastoma patients did not show a statistically significant increase in overall survival (OS). However, these trials did indicate a statistically significant improvement in progression-free survival (PFS) (7,8). Anti-VEGF treatments demonstrated that the enhancement on contrast-enhanced MRI was reduced, however, the outcome in patients was not improved with these treatments (9).

Piao et al. found that anti-VEGF therapy made tumors more resistant, invasive and aggressive, as the epithelial-to-mesenchymal transition took place (10). Lu et al. also showed that VEGF was able to regulate tumor invasiveness by recruiting protein tyrosine phosphatase 1B to MET/VEGFR2 heterocomplexes, which inhibited MET phosphorylation and tumor migration (11). In our previous research, increased glioma cell invasion due to anti-VEGF therapy was associated with extracellular matrix (ECM) changes, and an integrin inhibitor (cilengitide) reduced anti-VEGF therapy-induced glioma cell invasion (12).

The process of tumor cell invasion leads to the production of adhesion molecules and ECM. Studying the mechanism of bevacizumab-induced glioma invasion will help to develop novel glioma therapeutic strategies (13). In this study, we investigated the changes in expression of adhesion molecules in gliomas cells exposed to bevacizumab.

MATERIALS AND METHODS

Glioma cell line, drugs and transfection

The human glioma cell lines U87ΔEGFR, U251MG, A172, and Gli36 were prepared and maintained as described previously (14). Bevacizumab was provided by Genentech (San Francisco, CA, USA) /Roche (Basel, Switzerland) /Chugai Pharmaceutical Co (Tokyo, Japan).

The human glioblastoma-derived cancer stem cell line, MGG23 cells were provided by Dr Hiroaki Wakimoto at Massachusetts General Hospital. The human glioblastoma-derived cancer stem cell line, MGG23 cells were cultured as previously described (15,16). U87ΔEGFR, U251 and A172 were authenticated by Promega (Madison, WI, USA) via short tandem repeat profiling in December 2016. Mycoplasma is negative in all cells.

Ethics and animal use statement

This study was conducted in strict accordance to the recommendations in the Guide for the Care and Use of Laboratory Animals in Japan. All procedures and animal protocols were approved by the Committee on the Ethics of Animal Experimentation at Okayama University as described previously (12).

Brain xenografts

We prepared 1.0×10^5 U87ΔEGFR cells/ μ L as described previously (12). These cells were injected into athymic mice (balb/c-nu/nu; CLEA Japan, Inc.) or athymic rats (F344/N-nu/nu; CLEA Japan, Inc., Tokyo, Japan). Tumor cells were implanted into the right frontal lobe of athymic mice (2 μ L: 3 mm lateral and 1 mm anterior to the bregma at a depth of 3 mm) and athymic rats, as described previously. We administered PBS or bevacizumab (athymic mice or rats: 6 mg/kg) intraperitoneally, three times per week, starting on day 5 after tumor cell implantation.

We assessed the survival time of the U87ΔEGFR mouse glioma model using a Kaplan–Meier survival analysis.

Athymic animals were sacrificed at 18 days after tumor implantation, following six administrations of PBS or bevacizumab. The maximum transverse diameter of tumors was measured. Hematoxylin and eosin (HE) staining was performed as described previously (17).

qRT-PCR array analysis

Eighteen days after tumor implantation, U87ΔEGFR mouse models treated with bevacizumab or PBS were sacrificed (n=4 per group). RNA was extracted as previously described (10). RNA analysis was conducted with an Extracellular Matrix & Adhesion Molecules RT Profiler PCR Array (PAHS-013Z) (QIAGEN; Hilden, Germany), according to the manufacturer's instructions. Expression of genes encoding 84 human cell adhesion molecules and ECM components was evaluated in brain tumor tissue after bevacizumab treatment relative to control (PBS). We defined a gene as being upregulated when the bevacizumab treatment/control average intensity ratio was >2.0, and downregulated when the bevacizumab treatment/control ratio was <0.5. Data were extracted using the following criteria: P-value < 0.05. The array included controls to assess cDNA quality and DNA contamination. All data are deposited in the Gene Expression Omnibus (accession number GSE126168).

Quantitative reverse-transcription polymerase chain reaction (qRT-PCR)

We isolated total RNA from tumor cells incubated with bevacizumab (0, 1, 5, 10 and 100 µg/ml for 24 h) or PBS with an RNeasy Mini Kit (QIAGEN; Hilden, Germany). *In vivo*, total RNA was extracted from the brain tumor tissue of mice that had been treated with PBS or bevacizumab using the TRIzol reagent (Invitrogen, Carlsbad, CA, USA) as the manufacturer's instructions. qRT-PCR was performed as previously described (18). β-actin was used as an internal control.

We assessed gene expression of COL1A1 (Collagen, type I, alpha 1), ITGB2 (Integrin, beta 2 (complement component 3 receptor 3 and 4 subunit), VCAM1 (vascular cell adhesion molecule 1), and δ -catenin (CTNND2) (cadherin-associated protein, delta 2 [neural plakophilin-related arm-repeat protein]) in athymic mice harboring U87 Δ EGFR brain tumors

Primers were as follows: COL1A1: F (forward), 5'-cctggatgccatcaaagtct-3', R (reverse) 5'-gaatccatcggtcatgctct -3'; ITGB2 F (forward), 5'-gaccagagcattccaacacc -3', R (reverse), 5'-ttaaacggtttcaggaacg-3'; VCAM1 F (forward), 5'-attcactccgcggtatctg-3', R (reverse), 5'-ccaaggatcacgaccatctt -3'; CTNND2 F (forward), 5'-gccggaagtgattcagatgt -3', R (reverse), 5'-ctacggtggacttcggtcat -3'; and ACTB F (forward), 5'-agagctacgagctgcctgac -3', R (reverse), 5'-agcactgtgttgccgtacag-3'.

Immunohistochemistry

The avidin–biotin–peroxidase complex method (Ultrasensitive; MaiXin, Fuzhou, China) was performed for immunohistochemistry. δ -catenin mouse monoclonal antibody (1:300 dilution; Abcam, Inc., Cambridge, UK) was used for the staining. Mouse immunoglobulin was used as a negative control. Both antibodies were stained as previously described (15). Hematoxylin was used for counterstaining. We evaluated the positivity of cytoplasmic immunostaining in tumor cells.

Scratch wound assay

For scratch wound assays, data were collected at 6, 12, 18 and 24 h after scratching. We incubated cells to confluence using serum-starved DMEM. Scratches were made using a 200- μ L pipette tip and monolayer wounds were made. The medium was changed to DMEM containing either bevacizumab or vehicle (PBS). Glioma cells were assessed for movement after 18 h or 24 h of exposure to bevacizumab. Serum was starved during the assay.

Two-chamber assay

The invasion assay *in vitro* was performed using a 24-well plate and ThinCert (8 µm-pore, 24-well format, Greiner Bio-one; Kremsmunster, Austria) according to the manufacturer's instructions. The lower chamber was filled with DMEM with 10% FBS as a chemoattractant with or without 5 µg/mL bevacizumab. After a 24-hour incubation, non-invading cells were scraped from the top compartment. The insert filters were stained with 5% Giemsa solution. The number of invading cells was counted on the lower surface of the filter.

Matrigel invasion assay

The *in vitro* invasion assay was performed using 96-well ultra-low attachment wells (Corning, Inc.; New York, USA) according to the manufacturer's instructions. Briefly, 1×10^5 cells were seeded in low-serum DMEM in the bottom of wells. After a 24-h incubation, siRNAs were transfected into cells. After 24 h, bevacizumab or vehicle (PBS) was added to the wells, and subsequently Matrigel was added. Digital photomicrographs of the spheroid midplane were taken daily using with the BZ-8100 microscope (Keyence, Osaka, Japan). The radius of invasion was calculated using ImageJ (<http://rsb.info.nih.gov/ij/>), as previously described (19).

Water soluble tetrazolium-1 (WST-1) assay

The WST-1 assay was performed according to the manufacturer's protocol (Roche, Tokyo, Japan). Briefly, 2×10^3 cells in 100 µL of medium were placed in a 96-well microculture plate and incubated at 37 °C for 24-72hours. 10 µL of WST-1 solution was then added and cells were incubated for 4 h. Optical absorbance at a test wavelength of 450 nm and reference wavelength of 600 nm was measured with a microplate reader (Multiskan FC; Thermo Fisher Scientific, MA, USA).

Western blotting

Total cell protein was extracted in lysis buffer, and quantified using the Bradford method (20). Samples of 50 µg of protein were separated by SDS-PAGE. Samples were transferred to polyvinylidene fluoride membranes and incubated overnight at 4°C with anti- δ -catenin antibodies (1:1000; Abcam), anti-VEGFR2 antibodies (1:1000; Cell Signaling Technology, Danvers, MA, USA) and a mouse monoclonal antibody against β -actin (1:5,000; Sigma, St. Louis, MO, USA). The membrane was incubated with HRP-conjugated appropriate secondary antibodies for 1 h. Immunoreactive bands were visualized using the ECL Prime Western Blotting Detection Reagent (GE Healthcare; Tokyo, Japan) and the VersaDoc 5000 MP (Bio-Rad Laboratories; CA, USA). We quantified relative protein levels using β -actin as a loading control.

siRNA and shRNA transfection

Lipofectamine 3000 transfection reagent (Thermo Fisher Scientific, MA, USA) was used for transfection of small interfering RNAs (siRNAs) into U87 Δ EGFR cell lines, according to the manufacturer's instructions. The δ -catenin siRNA sequence was #1:5'- UCG CCU CAG UCA AAG AAC AGG AAU U -3'; and #2: 5'-CCC ACA GGA UUA UUC UAC AGG UGA A-3'. A nonsilencing siRNA sequence was used as a negative control (Thermo Fisher Scientific Inc. [Waltham, MA; Dharmacon, Stealth RNAi siRNA]). Protein levels were assessed after 48 h using western blotting. Targeted downregulation of δ -catenin in U87 Δ EGFR cells was achieved by transfection of an siRNA targeted to δ -catenin (5'-(UCU CGA GCU GGU GGA CUC CUG UAU U)-3') (ThermoFisher Scientific; Yokohama, Japan), according to the manufacturer's instructions.

Human δ -catenin plasmids were purchased from GeneCopoeia (Cat.No.LPP-ProdId-LV202-050, Rockville, MD, USA). The lentivirus encoding Human δ -catenin plasmids, scramble short hairpin RNA (shRNA) and shRNA against human δ -catenin and VEGFR2 were prepared using the pLKO.1, psPAX2 and pMD2.G plasmids (Addgene,

Cambridge, CA); 293FT cells; and the FuGENE6 Transfection Reagent (Promega, Madison, WI) according to manufacturer's recommendation. The shRNA sequences against human VEGFR2 were as follows:

shVEGFR2#1:

5'-CCGGCCACAGATCATGTGGTTTAAACTCGAGTTTAAACCACATGATCTGTGGTTTTT-3'; and

shVEGFR2#2:

5'-CCGGCTGGAATGAATACCCTCATATCTCGAGATATGAGGGTATTCATTCCAGTTTTT-3'.

RESULTS

Effect of bevacizumab treatment in xenograft mouse or rat models

The antitumor effect of bevacizumab was tested in animals harboring intracerebral U87 Δ EGFR glioma cells. The survival time of mice treated with bevacizumab was longer than that of control mice (median survival = 17.5 and 26 days, respectively; $p=0.0033$; Fig 1A).

As assessed using the maximum transverse diameter, tumor volume was lower in the brains of rats treated with bevacizumab compared with untreated controls at 18 days after tumor inoculation ($p=0.0209$; Fig. 1B).

The mouse glioma model with U87 Δ EGFR cells showed angiogenic growth and well-demarcated borders in the brain (Fig. 1C, a). However, anti-VEGF therapy with bevacizumab increased cell invasion (Fig 1C, b). In the mouse model, we observed similar histological results to previous rat data (12).

qRT-PCR array analysis of the effect of bevacizumab therapy on the U87 Δ EGFR mouse model

To illustrate the molecular mechanisms related to the anti-VEGF treatment invasiveness, gene expression in tumor tissues was compared between U87 Δ EGFR orthotopic mice in the bevacizumab and the control. The resultant plot arranges genes according to their biologic and

statistical significance (Fig. 1D). Several genes exhibited differential expression in bevacizumab-treated U87ΔEGFR glioma tissue compared with control U87ΔEGFR glioma tissue, comprising 11 upregulated genes (Table 1A) and four downregulated genes (Table 1B). For the upregulated genes, the following 11 genes were identified: δ-catenin, VCAM1, ITGB2, MMP7, MMP1, ITGA8, ANOS1, HGDC, TGFBI, COL1A1, and COL4A2. For the downregulated genes, the following four were identified: LAMA2, HAS1, VTN, and ITGA7.

Validation of the qRT-PCR array results

To confirm the results from the qRT-PCR array analysis, COL1A1, ITGB2, VCAM1 and δ-catenin, which are associated with the ECM, adhesion molecules and tumor cell invasion, were verified using qRT-PCR analysis. Relative expression levels of COL1A1, VCAM1, ITGB2, and δ-catenin in the U87ΔEGFR mouse model with bevacizumab were upregulated compared with the control group, by 3.24-fold, 1.59-fold, 2.38-fold, and 16.5-fold, respectively ($p < 0.05$; Fig. 1E). δ-catenin expression was markedly elevated.

δ-catenin expression in a glioma model

Using immunohistochemistry, bevacizumab treatment led to high δ-catenin expression in U87ΔEGFR cells compared with the control group (Fig. 1F). δ-catenin was expressed at the invasive tumor border in the mouse glioma model of U87ΔEGFR cells. These data indicate that δ-catenin is related to bevacizumab-induced glioma invasion in an *in vivo* glioma model.

Glioma cell cytotoxicity and migration with bevacizumab treatment in vitro

We investigated the cytotoxic effect of bevacizumab on glioma cells *in vitro*. Incubation with bevacizumab for the indicated time did not alter the glioma cell proliferation rate (Supplementary Figure 1).

Wound closure was significantly enhanced by bevacizumab (Fig. 2A, Supplementary

Figure 2). Low-dose bevacizumab also elevated the motility of U251MG, A172, Gli36 cell lines (Fig. 2B). This assay indicated that bevacizumab treatment influences glioma cell migration.

δ-catenin expression in vitro

δ-catenin expression was also confirmed by qRT-PCR and western blot *in vitro*. Relative expression of δ-catenin in U87ΔEGFR cells treated with bevacizumab was increased by 23-fold compared with controls ($p < 0.05$; Fig. 2C). In western blotting, δ-catenin protein expression was augmented in a dose-dependent manner (Fig. 2D). The expression of δ-catenin was also increased in U251MG, A172, and Gli36 glioma cell lines compared with untreated cells (Fig. 2E).

Migration behavior of δ-catenin overexpressed tumor cells

We established a δ-catenin overexpressed tumor cell line after lentivirus transfection of U87ΔEGFR cells. δ-catenin was upregulated by δ-catenin overexpressed transfection compared with control. Expression levels of COL1A1, VCAM1 were also upregulated, but ITGB2 was not significantly changed by δ-catenin overexpressed transfection (Fig. 3A).

δ-catenin expression levels were confirmed using western blotting analysis (Fig. 3B). In the two-chamber assay, δ-catenin-overexpressing U87ΔEGFR cells were more invasive compared with the control (Fig. 3C, $*p < 0.05$). Mice in the δ-catenin-overexpressed cells group showed unclear tumor borders. We assessed the depth of invasion from the tumor border to the invading cells. The depth of tumor invasion in the U87ΔEGFR cells expressing δ-catenin was significantly increased compared with empty vector-transfected U87ΔEGFR cells (Fig. 3D). δ-catenin overexpression was confirmed at the invasive tumor border in the mouse orthotopic glioma model with overexpressing δ-catenin U87ΔEGFR cells (Supplementary Figure 3).

Migration behavior after anti-δ-catenin siRNA transfection to tumor cell line

δ -catenin expression levels were confirmed by qRT-PCR analysis after siRNA transfection of U87 Δ EGFR cells. Relative expression of δ -catenin in U87 Δ EGFR cells transfected with the δ -catenin siRNA was decreased compared with bevacizumab-treated cells ($p < 0.05$; Fig. 4A). Western blotting data also showed that U87 Δ EGFR (Fig. 4B,C) and glioma stem cell (GSC, MGG23; Fig. 4D) δ -catenin levels were lower after siRNA or shRNA transfection than bevacizumab incubation. COL1A1, ITGB2, and VCAM1 expression patterns were examined when δ -catenin was knocked down. COL1A1, ITGB2, and VCAM1 expression levels were detected (Fig. 4E). In the scratch assay, U87 Δ EGFR cells harboring the δ -catenin siRNA were less invasive than bevacizumab-treated cells (Fig. 4F, G * $p < 0.05$, ** $p < 0.01$). Moreover, in the two-chamber invasion assay, U87 Δ EGFR were less invasive after transfection of the δ -catenin shRNA compared with bevacizumab incubation (Fig. 4H, I).

Effect of bevacizumab treatment in xenograft mouse model of U87 Δ EGFR cells expressing δ -catenin shRNA

Matrigel invasion assays showed that δ -catenin siRNA transfection inhibited bevacizumab-induced glioma cell invasion (Fig. 5A; U87 Δ EGFR, B; MGG23).

Moreover, we made U87 Δ EGFR cells expressing δ -catenin shRNA or scramble shRNA and implanted each cell type into the brain of athymic mice. Tumors in the PBS group showed well-defined borders (Fig. 5C, a), while bevacizumab-treated cells expressing scramble shRNA consistently invaded normal brains and the tumor border became irregular (Fig. 5C, b). The invasion depth in the U87 Δ EGFR expressing δ -catenin shRNA samples treated with bevacizumab was significantly less compared to U87 Δ EGFR expressing scramble shRNA treated with bevacizumab group (Fig. 5D; $p < 0.05$). Decreased δ -catenin expression was confirmed at the tumor in the mouse orthotopic glioma model with δ -catenin-knockdown U87 Δ EGFR cells treated with bevacizumab (Supplementary Figure 3). We made VEGFR-knockdown GBM cells using shRNA against human VEGFR2. The δ -catenin

expression level was not changed when VEGFR2 was knocked down. Cell viability and migrating cells were decreased (Supplementary Figure 4). Invasion cells under bevacizumab treatment were also decreased when VEGFR2 was knocked down (Fig. 5E).

DISCUSSION

This study demonstrated that anti-VEGF therapy prolonged the overall survival of mice. In the glioma orthotopic models, bevacizumab treatment inhibited angiogenesis, but promoted tumor invasion. Analysis on qRT-PCR arrays of xenograft tumor cells demonstrated that bevacizumab alters gene expression of some ECM and adhesion molecules. qPCR array analysis in the U87ΔEGFR orthotopic mouse model showed that bevacizumab led to upregulation of COL1A1, VCAM1, ITGB, and δ -catenin (CTNND2). This observation affirmed the previously reported findings that bevacizumab increases perivascular ECM in tumors containing collagen fibers (12). δ -catenin gene expression was potently upregulated. In this study, δ -catenin was associated with bevacizumab-induced glioma invasion *in vivo* and *in vitro*.

Bevacizumab-induced glioma invasion

Previously, we showed a decreasing the number of vessels in the tumor xenograft model (10), and we demonstrated prolonged survival when treated with bevacizumab. The VEGF autocrine signaling loop is suppressed, the Akt and Erk pathways are activated, and tumor growth and invasion are stimulated by anti-VEGF therapy (21). Molecules within the ECM microenvironment such as proteoglycans and collagens may influence the process of tumor invasion during anti-VEGF therapy (22).

δ -catenin upregulation in bevacizumab-induced glioma model

Cell-cell adhesion molecules include the cadherin family and the immunoglobulin superfamily (IgSF). Cell-matrix adhesion molecules include the integrin family and components of the ECM

fibronectin, laminin, collagen, tenascin, BAI1 (brain specific angiogenesis inhibitor), CCN1 (cysteine-rich 61/connective tissue growth factor/ nephroblastoma overexpressed) and proteoglycans (3,18,23-30). Comprehensive analysis of adhesion molecules by qRT-PCR array revealed upregulated expression of the δ -catenin gene. By qRT-PCR array analysis, anti-VEGF therapy increased gene expression of COL1A1, VCAM, ITGB2 and δ -catenin compared with the control group. These data reflect the underlying mechanisms of bevacizumab-induced glioma invasion. The fold-change in expression was markedly higher for δ -catenin than the other genes.

δ -catenin is a member of the p120 subfamily, and these proteins are almost solely expressed in nervous system structures. δ -catenin is crucially associated with nervous system functions such as neurite elongation and dendritic morphogenesis (31,32). δ -catenin belongs to the p120 catenin subgroup. p120 catenin binds to E-cadherin at the proximal membrane side, regulating cell growth through stimulation of c-Src (33), and affects cell motility via changes to the cytoskeleton through actin filament movements (34). δ -catenin was discovered because it is able to bind to presenilin-1 (35) that was related to mutated genes found in familial Alzheimer's disease (36). δ -catenin plays a significant role in dendritic morphogenesis, which is related to changes in small GTPase activity.

For the relationship between δ -catenin and other ECM molecules, we showed an upregulation of COL1A1 with over-expression of δ -catenin, but even with δ -catenin knockdown, COL1A1 was still upregulated. Although little is known about the relationship between COL1A1 and δ -catenin, δ -catenin binds to E-cadherin (37) and cadherin is associated with COL1A1 (38). Moreover, the expression of another type of catenin, β -catenin, was reported to result in spontaneous, progressive skin fibrosis with thickened collagen fibers (39). In stabilized β -catenin cells, there was an increase in the relative expression of COL1A1 mRNA. The relationship between δ -catenin and COL1A1 may occur through a similar mechanism as that of β -catenin. However, δ -catenin binds to E-cadherin in a competitive manner with p120 catenin

(37). For δ -catenin knockdown, p120 catenin might bind to cadherin and induce COL1A1 upregulation. Further studies on the detailed mechanisms of the relationship between δ -catenin and other ECM molecules are required.

Role of δ -catenin in glioma

δ -catenin is strongly expressed in the normal brain, especially in neurons. Mutations in the δ -catenin gene, which loses its function in mesenchymal glioblastoma, might be the key event that causes aggressiveness in this glioblastoma subtype (40). The δ -catenin mutations are associated with transformation of the glioma into a very aggressive mesenchymal phenotype. We used the IVY glioblastoma atlas project database and showed that δ catenin is highly expressed at the tumor edge and in the infiltrating tumor (Fig. 5F). δ -catenin might be associated with astrocytoma progression and could be a potential biomarker for the behavior of astrocytoma cells (41). In this study, we showed that δ -catenin expression was upregulated by low concentrations of bevacizumab *in vitro* and in a bevacizumab-induced invasive model *in vivo*.

Association between δ -catenin and bevacizumab-induced glioma invasion

siRNA and shRNA-mediated knockdown of δ -catenin in U87 Δ EGFR cells markedly decreased bevacizumab-induced cell invasion. δ -catenin was reported to promote the invasion of colorectal cancer cells by binding to E-cadherin in a competitive manner with p120 catenin (37). δ -catenin was found to stimulate astrocytoma cell invasion through upregulation of Rac1 activity(41). Therefore, δ -catenin is strongly associated with tumor cell invasion.

It has been reported that VEGF directly and negatively regulates tumor cell invasion (42,43). The main VEGF signaling circuit is VEGFR2, which is related to all critical endothelial functions such as proliferation, migration, and vessel formation (44-46). VEGF binding to VEGFR2 has also been reported to inhibit invasiveness (43). In our VEGFR-knockdown

experiment δ -catenin expression level was unchanged. However, invasion cells under bevacizumab treatment were decreased. There is a possibility of different routes of bevacizumab induced invasion. Further information about the detailed mechanisms of the relationship between the VEGF pathway and δ -catenin is required.

CONCLUSION

This study showed that some ECM factors were altered and that anti-VEGF therapy induced glioma cell invasion. The findings suggest that δ -catenin is implicated in bevacizumab-induced glioma cell invasion.

Statistical analysis

The Student's *t*-test and ANOVA were used to test for statistical significance. Data are presented as the mean \pm standard deviation (SD) and standard error (SE). Differences were considered to denote statistical significance when $p < 0.05$. All statistical analyses were performed using SPSS statistical software, version 20 (SPSS, Inc., Chicago, IL, USA).

Abbreviations

ANOS1, anosmin 1; COL1A1, collagen, type I, alpha 1; COL4A2, collagen, type IV, alpha 2; δ -catenin, CTNND2 (cadherin-associated protein, delta 2 (neural plakophilin-related arm-repeat protein)); HAS1, hyaluronan synthase 1; HGDC, (R)-hydroxyglutaryl-CoA dehydratase activator; ITGA7, integrin, alpha 7; ITGA8, integrin, alpha 8; ITGB2, Integrin, beta 2; LAMA2, laminin, alpha 2; MMP1, matrix metalloproteinase 1; MMP7, matrix metalloproteinase-7; TGFBI, transforming growth factor, beta induced; VCAM1, vascular cell adhesion molecule 1; VTN, vitronectin

Acknowledgments

We would like to thank M. Arao, N. Uemori, and Y. Ukai for their technical assistance. The following medical students also contributed to the animal experiments: Y. Inoue. Bevacizumab was generously provided by Genentech/Roche/Chugai Pharmaceutical Co. We thank Jodi Smith, PhD, from Edanz Group (www.edanzediting.com/ac) for editing a draft of this manuscript.

References

1. Stupp R, Mason WP, van den Bent MJ, Weller M, Fisher B, Taphoorn MJ, *et al.* Radiotherapy plus concomitant and adjuvant temozolomide for glioblastoma. *N Engl J Med* **2005**;352(10):987-96 doi 10.1056/NEJMoa043330.
2. Touat M, Idbaih A, Sanson M, Ligon KL. Glioblastoma targeted therapy: updated approaches from recent biological insights. *Annals of oncology : official journal of the European Society for Medical Oncology* **2017**;28(7):1457-72 doi 10.1093/annonc/mdx106.
3. Kurozumi K, Ichikawa T, Onishi M, Fujii K, Date I. Cilengitide treatment for malignant glioma: current status and future direction. *Neurologia medico-chirurgica* **2012**;52(8):539-47.
4. Bokstein F, Shpigel S, Blumenthal DT. Treatment with bevacizumab and irinotecan for recurrent high-grade glial tumors. *Cancer* **2008**;112(10):2267-73 doi 10.1002/cncr.23401.
5. Vredenburgh JJ, Desjardins A, Herndon JE, 2nd, Marcello J, Reardon DA, Quinn JA, *et al.* Bevacizumab plus irinotecan in recurrent glioblastoma multiforme. *Journal of clinical oncology : official journal of the American Society of Clinical Oncology* **2007**;25(30):4722-9 doi 10.1200/JCO.2007.12.2440.
6. Dvorak HF. Vascular permeability factor/vascular endothelial growth factor: a critical cytokine in tumor angiogenesis and a potential target for diagnosis and therapy. *Journal of clinical oncology : official journal of the American Society of Clinical Oncology* **2002**;20(21):4368-80.
7. Chinot OL, Wick W, Mason W, Henriksson R, Saran F, Nishikawa R, *et al.* Bevacizumab plus radiotherapy-temozolomide for newly diagnosed glioblastoma. *N Engl J Med* **2014**;370(8):709-22 doi 10.1056/NEJMoa1308345.
8. Gilbert MR, Dignam JJ, Armstrong TS, Wefel JS, Blumenthal DT, Vogelbaum MA, *et al.* A randomized trial of bevacizumab for newly diagnosed glioblastoma. *N Engl J Med* **2014**;370(8):699-708 doi 10.1056/NEJMoa1308573.
9. Desjardins A, Reardon DA, Herndon JE, 2nd, Marcello J, Quinn JA, Rich JN, *et al.* Bevacizumab plus irinotecan in recurrent WHO grade 3 malignant gliomas. *Clinical cancer research : an official journal of the American Association for Cancer Research* **2008**;14(21):7068-73 doi 10.1158/1078-0432.CCR-08-0260.
10. Piao Y, Liang J, Holmes L, Zurita AJ, Henry V, Heymach JV, *et al.* Glioblastoma resistance to anti-VEGF therapy is associated with myeloid cell infiltration, stem cell accumulation, and a mesenchymal phenotype. *Neuro Oncol* **2012**;14(11):1379-92 doi 10.1093/neuonc/nos158.
11. Lu KV, Chang JP, Parachoniak CA, Pandika MM, Aghi MK, Meyronet D, *et al.* VEGF inhibits tumor cell invasion and mesenchymal transition through a MET/VEGFR2 complex. *Cancer Cell* **2012**;22(1):21-35 doi 10.1016/j.ccr.2012.05.037.
12. Ishida J, Onishi M, Kurozumi K, Ichikawa T, Fujii K, Shimazu Y, *et al.* Integrin inhibitor suppresses bevacizumab-induced glioma invasion. *Transl Oncol* **2014**;7(2):292-302 e1 doi 10.1016/j.tranon.2014.02.016.
13. Shimizu T, Kurozumi K, Ishida J, Ichikawa T, Date I. Adhesion molecules and the extracellular matrix as drug targets for glioma. *Brain Tumor Pathol* **2016**;33(2):97-106 doi 10.1007/s10014-016-0261-9.
14. Kambara H, Okano H, Chiocca EA, Saeki Y. An oncolytic HSV-1 mutant expressing ICP34.5 under control of a nestin promoter increases survival of animals even when symptomatic from a brain tumor. *Cancer research* **2005**;65(7):2832-9 doi 10.1158/0008-5472.CAN-04-3227 [pii] 10.1158/0008-5472.CAN-04-3227.
15. Wakimoto H, Kesari S, Farrell CJ, Curry WT, Zaupa C, Aghi M, *et al.* Human

- glioblastoma–derived cancer stem cells: establishment of invasive glioma models and treatment with oncolytic herpes simplex virus vectors. *Cancer research* **2009**;69(8):3472-81.
16. Wakimoto H, Mohapatra G, Kanai R, Curry WT, Yip S, Nitta M, *et al.* Maintenance of primary tumor phenotype and genotype in glioblastoma stem cells. *Neuro-oncology* **2011**;14(2):132-44.
 17. Onishi M, Ichikawa T, Kurozumi K, Fujii K, Yoshida K, Inoue S, *et al.* Bimodal anti-glioma mechanisms of cilengitide demonstrated by novel invasive glioma models. *Neuropathology : official journal of the Japanese Society of Neuropathology* **2013**;33(2):162-74 doi 10.1111/j.1440-1789.2012.01344.x.
 18. Kurozumi K, Hardcastle J, Thakur R, Yang M, Christoforidis G, Fulci G, *et al.* Effect of tumor microenvironment modulation on the efficacy of oncolytic virus therapy. *J Natl Cancer Inst* **2007**;99(23):1768-81 doi 10.1093/jnci/djm229.
 19. Young N, Pearl DK, Van Brocklyn JR. Sphingosine-1-phosphate regulates glioblastoma cell invasiveness through the urokinase plasminogen activator system and CCN1/Cyr61. *Molecular cancer research* **2009**;7(1):23-32.
 20. Li H, Zhang Y, Zhang Y, Bai X, Peng Y, He P. Rsf-1 overexpression in human prostate cancer, implication as a prognostic marker. *Tumor Biology* **2014**;35(6):5771-6.
 21. Simon T, Coquerel B, Petit A, Kassim Y, Demange E, Le Cerf D, *et al.* Direct effect of bevacizumab on glioblastoma cell lines in vitro. *Neuromolecular Med* **2014**;16(4):752-71 doi 10.1007/s12017-014-8324-8.
 22. de Groot JF, Fuller G, Kumar AJ, Piao Y, Eterovic K, Ji Y, *et al.* Tumor invasion after treatment of glioblastoma with bevacizumab: radiographic and pathologic correlation in humans and mice. *Neuro Oncol* **2010**;12(3):233-42 doi 10.1093/neuonc/nop027.
 23. Fujii K, Kurozumi K, Ichikawa T, Onishi M, Shimazu Y, Ishida J, *et al.* The integrin inhibitor cilengitide enhances the anti-glioma efficacy of vasculostatin-expressing oncolytic virus. *Cancer gene therapy* **2013**;20(8):437-44 doi 10.1038/cgt.2013.38.
 24. Ishida J, Kurozumi K, Ichikawa T, Otani Y, Onishi M, Fujii K, *et al.* Evaluation of extracellular matrix protein CCN1 as a prognostic factor for glioblastoma. *Brain Tumor Pathol* **2015**;32(4):245-52 doi 10.1007/s10014-015-0227-3.
 25. Kaur B, Brat DJ, Devi NS, Van Meir EG. Vasculostatin, a proteolytic fragment of brain angiogenesis inhibitor 1, is an antiangiogenic and antitumorigenic factor. *Oncogene* **2005**;24(22):3632-42.
 26. Kurozumi K, Hardcastle J, Thakur R, Shroll J, Nowicki M, Otsuki A, *et al.* Oncolytic HSV-1 infection of tumors induces angiogenesis and upregulates CYR61. *Molecular therapy : the journal of the American Society of Gene Therapy* **2008**;16(8):1382-91 doi 10.1038/mt.2008.112 [pii]
 27. Onishi M, Kurozumi K, Ichikawa T, Date I. Mechanisms of tumor development and anti-angiogenic therapy in glioblastoma multiforme. *Neurologia medico-chirurgica* **2013**;53(11):755-63.
 28. Onishi M, Kurozumi K, Ichikawa T, Michiue H, Fujii K, Ishida J, *et al.* Gene expression profiling of the anti-glioma effect of Cilengitide. *SpringerPlus* **2013**;2(1):160 doi 10.1186/2193-1801-2-160.
 29. Shimazu Y, Kurozumi K, Ichikawa T, Fujii K, Onishi M, Ishida J, *et al.* Integrin antagonist augments the therapeutic effect of adenovirus-mediated REIC/Dkk-3 gene therapy for malignant glioma. *Gene therapy* **2015**;22(2):146-54 doi 10.1038/gt.2014.100.
 30. Otani Y, Ishida J, Kurozumi K, Oka T, Shimizu T, Tomita Y, *et al.* PIK3R1Met326Ile germline mutation correlates with cysteine-rich protein 61 expression and poor prognosis in glioblastoma. *Scientific reports* **2017**;7(1):7391.
 31. Arikath J, Peng IF, Ng YG, Israely I, Liu X, Ullian EM, *et al.* Delta-catenin regulates

- spine and synapse morphogenesis and function in hippocampal neurons during development. *The Journal of neuroscience : the official journal of the Society for Neuroscience* **2009**;29(17):5435-42 doi 10.1523/jneurosci.0835-09.2009.
32. Kosik KS, Krichevsky AM. Teaching resources. A model for local regulation of translation near active synapses. *Science's STKE : signal transduction knowledge environment* **2005**;2005(300):tr25 doi 10.1126/stke.3002005tr25.
 33. Abu-Elneel K, Ochiishi T, Medina M, Remedi M, Gastaldi L, Caceres A, *et al.* A delta-catenin signaling pathway leading to dendritic protrusions. *The Journal of biological chemistry* **2008**;283(47):32781-91 doi 10.1074/jbc.M804688200.
 34. Reynolds AB, Rocznik-Ferguson A. Emerging roles for p120-catenin in cell adhesion and cancer. *Oncogene* **2004**;23(48):7947-56 doi 10.1038/sj.onc.1208161.
 35. Zhou J, Liyanage U, Medina M, Ho C, Simmons AD, Lovett M, *et al.* Presenilin 1 interaction in the brain with a novel member of the Armadillo family. *Neuroreport* **1997**;8(8):2085-90.
 36. Sherrington R, Rogaev EI, Liang Y, Rogaeva EA, Levesque G, Ikeda M, *et al.* Cloning of a gene bearing missense mutations in early-onset familial Alzheimer's disease. *Nature* **1995**;375(6534):754-60 doi 10.1038/375754a0.
 37. Zhang H, Dai SD, Zhang D, Liu D, Zhang FY, Zheng TY, *et al.* Delta-catenin promotes the proliferation and invasion of colorectal cancer cells by binding to E-cadherin in a competitive manner with p120 catenin. *Targeted oncology* **2014**;9(1):53-61 doi 10.1007/s11523-013-0269-6.
 38. Liu J, Eischeid AN, Chen X-M. Col1A1 production and apoptotic resistance in TGF- β 1-induced epithelial-to-mesenchymal transition-like phenotype of 603B cells. *PloS one* **2012**;7(12):e51371.
 39. Hamburg-Shields EJ. Roles of beta-catenin in dermal fibrosis: Case Western Reserve University; 2015.
 40. Frattini V, Trifonov V, Chan JM, Castano A, Lia M, Abate F, *et al.* The integrated landscape of driver genomic alterations in glioblastoma. *Nat Genet* **2013**;45(10):1141-9 doi 10.1038/ng.2734.
 41. Wang M, Dong Q, Zhang D, Wang Y. Expression of delta-catenin is associated with progression of human astrocytoma. *BMC Cancer* **2011**;11:514 doi 10.1186/1471-2407-11-514.
 42. Sennino B, Ishiguro-Oonuma T, Wei Y, Naylor RM, Williamson CW, Bhagwandin V, *et al.* Suppression of tumor invasion and metastasis by concurrent inhibition of c-Met and VEGF signaling in pancreatic neuroendocrine tumors. *Cancer discovery* **2012**.
 43. Lu KV, Chang JP, Parachoniak CA, Pandika MM, Aghi MK, Meyronet D, *et al.* VEGF inhibits tumor cell invasion and mesenchymal transition through a MET/VEGFR2 complex. *Cancer cell* **2012**;22(1):21-35.
 44. Ferrara N, Gerber H-P, LeCouter J. The biology of VEGF and its receptors. *Nature medicine* **2003**;9(6):669.
 45. Olsson A-K, Dimberg A, Kreuger J, Claesson-Welsh L. VEGF receptor signalling? In control of vascular function. *Nature reviews Molecular cell biology* **2006**;7(5):359.
 46. Shibuya M. Differential roles of vascular endothelial growth factor receptor-1 and receptor-2 in angiogenesis. *BMB Reports* **2006**;39(5):469-78.

Table 1A Upregulated genes in bevacizumab treated group

Gene Symbol	Log2 Fold Regulation (test/control)	p-value
δ -catenin	6.54	0.031024
VCAM1	3.68	0.028437
ITGB2	3.19	0.002898
MMP7	2.83	0.000031
MMP1	2.26	0.002229
ITGA8	2.21	0.022767
ANOS1	2.07	0.041709
HGDC	2.07	0.041709
TGFBI	1.51	0.021752
COL1A1	1.34	0.002345
COL4A2	1.08	0.004979

Table 1B Down-regulated genes in bevacizumab treated group

Gene Symbol	Log2 Fold Regulation (test/control)	p-value
LAMA2	-1.32	0.004042
HAS1	-1.12	0.016108
VTN	-1.11	0.002552
ITGA7	-1.02	0.02621

Figure legends

Figure 1

Effect of bevacizumab treatment in xenograft mouse or rat models. (A) Kaplan–Meier survival curves of the U87ΔEGFR mouse glioma models treated with bevacizumab. Vehicle or bevacizumab (for the athymic mice: 6 mg/kg) was administered intraperitoneally three times per week, starting on day 5 after tumor cell implantation. The median survival time of mice treated with bevacizumab (27 days) was longer than that of the control group (16 days; $p=0.0136$, statistical significance was calculated by log-rank test). (B) Athymic rats harboring U87ΔEGFR brain tumors were sacrificed at 18 days after tumor implantation and six doses of vehicle or bevacizumab were administered ($n = 4$). Measurement of the maximum transverse tumor diameter revealed that tumor volume was lower in rats treated with bevacizumab compared with vehicle controls ($p=0.0209$. Statistical significance was calculated by the ANOVA with Turkey's *post-hoc* test). (C) a: The borders with brain tissue were well defined in an untreated U87ΔEGFR orthotopic mouse tumor. b: Invasion of tumor cells with vessel co-option in a bevacizumab-treated mouse tumor, which is consistent with previously shown invasive behavior in a rat model.

qPCR array analysis of the effect of bevacizumab treatment and δ -catenin expression in glioma model. (D) There were 11 differentially expressed genes between the bevacizumab group (Bev) and the control group, and four downregulated genes ($*p < 0.05$; mean \pm SE, $n = 3$). RQ, relative quantification. (E) Expression levels of COL1A1, VCAM1, ITGB2 and δ -catenin were increased by bevacizumab compared with vehicle control ($*p<0.05$) (mean \pm SE, $n = 3$). RQ, relative quantification. Statistical significance was calculated using the Student *t*-test. (F) Immunohistochemistry showed that bevacizumab-treated U87ΔEGFR cells expressed high levels of δ -catenin compared with controls both in the tumor center and at the invasive tumor border. Scale bar: 200 μ m (C), 100 μ m (F).

Figure 2

Glioma cells were assayed for movement after 18h and 24 h of exposure to bevacizumab.

Low-dose bevacizumab increased the motility of glioma cells in scratch wound assays. (A) a: Under 5- $\mu\text{g/ml}$ of bevacizumab condition, U87 Δ EGFR cell motility was increased in scratch wound assays. b: Representative images from scratch wound assays, in which glioma cell motility was monitored after 24 h of bevacizumab exposure. (B) Low-dose bevacizumab also increased the motility of U251MG, A172, Gli36 cell line. Scale bar, 200 μm

Upregulation of δ -catenin by treatment with bevacizumab in qRT-PCR and western blotting *in vitro*. (C) qRT-PCR demonstrated that δ -catenin was upregulated by a low concentration of bevacizumab ($p < 0.05$). (D) a: In U87 Δ EGFR glioma cells, the increase in protein expression of δ -catenin was greater after bevacizumab treatment than control. b: Quantification of the expression ratio (average expression levels: 1 $\mu\text{g/ml}$; 1.61, 5 $\mu\text{g/ml}$; 2.23, 10 $\mu\text{g/ml}$; 2.35; $p < 0.05$). (E) In other several glioma cell lines (U251MG, A172, Gli36), δ -catenin was upregulated by a low concentration of bevacizumab. Protein band density was calculated using ImageJ software. Data are presented as the mean \pm SD. Statistical significance was calculated using the Student's *t*-test for (A), (B), and (C), and ANOVA with Dunnett's test for (D). * $p < 0.05$. Scale bar, 100 μm (A).

Figure 3

δ -catenin overexpressed transfection to tumor cell line. (A) In qRT-PCR, δ -catenin (55-fold) was upregulated by δ -catenin overexpressed transfection compared with control. Expression levels of COL1A1 (26 fold), VCAM1 (12 fold) were upregulated by δ -catenin overexpressed transfection compared with control (* $p < 0.05$). ITGB2 was not significantly changed (mean \pm SE, $n = 3$). RQ, relative quantification. Statistical significance was calculated by the Student's T-test.

* $p < 0.05$. (B) The expression of δ -catenin was increased by δ -catenin overexpressed transfection. (C) In the two-chamber assay, δ -catenin-overexpressed U87 Δ EGFR cells were more invasive than empty vector-transfected cells ($p < 0.05$). (D) Mice in the δ -catenin overexpressed cells group (a) showed unclear tumor borders compared with control (b). (c) The depth of tumor invasion in the U87 Δ EGFR cells expressing δ -catenin was significantly increased compared with control. Scale bar, 100 μm . Values are presented as the mean \pm SE from three independent experiments. Statistical significance was calculated using ANOVA with Tukey's *post-hoc* test (* $p < 0.05$). Scale bar, 50 μm (C), 200 μm (D).

Figure 4

Anti- δ -catenin siRNA transfection to tumor cell line. (A) In qRT-PCR, δ -catenin was upregulated by a low concentration of bevacizumab ($p < 0.05$), and δ -catenin siRNA transfection suppressed δ -catenin expression (A). In U87 Δ EGFR glioma cells and glioma stem cells (MGG23), the bevacizumab-induced increase in δ -catenin protein expression was decreased by δ -catenin siRNA and shRNA knockdown (B-D). The expression patterns of COL1A1, ITGB2, VCAM1 were examined when δ -catenin is knocked down. Expression levels of COL1A1 was increased compared with δ -catenin sh scramble. Expression levels of VCAM1 and ITGB2 δ -catenin were decreased compared with δ -catenin sh scramble (E). (mean \pm SE, $n = 3$)

Migration behavior after anti- δ -catenin siRNA transfection into the tumor cell line. U87 Δ EGFR cells were serum-starved for 24 h, treated with bevacizumab (0, 1, 5, 10, or 100 $\mu\text{g}/\text{ml}$), and processed for scratch wound healing assays. δ -catenin siRNA transfection inhibited bevacizumab-induced glioma cell invasion (F,G). In the two-chamber assay, the invasiveness was decreased in U87 Δ EGFR transfected with lentivirus encoding δ -catenin shRNA ($n=6$) compared with U87 Δ EGFR transfected with lentivirus encoding scramble shRNA ($n=6$). The invasiveness was decreased in U87 Δ EGFR transfected with lentivirus encoding δ -catenin shRNA under bevacizumab treatment condition ($n=6$), (H,I). * $p < 0.05$

Scale bar, 100 μm (F), 50 μm (H). Values are the mean \pm SE from three independent experiments. Statistical significance was calculated using an ANOVA with Tukey's *post-hoc* test for (A), (C), (G), and (I), and the Student's *t*-test for (E). * $p < 0.05$

Figure 5

Matrigel invasion assays showed that δ -catenin shRNA transfection inhibited bevacizumab-induced glioma cell invasion (A; U87 Δ EGFR, B; MGG23).

We sacrificed athymic mice at 18 days after tumor implantation and PBS or bevacizumab was administered six times (C). a: PBS-treated U87 Δ EGFR orthotopic mouse tumor borders were demarcated in the normal brain; b: In a bevacizumab-treated tumor, cell invasion was increased; c: Silencing of δ -catenin decreased bevacizumab-induced glioma cell invasion. In U87 Δ EGFR expressing scramble shRNA treated with bevacizumab, the mean depth of tumor invasion was $350 \pm 63 \mu\text{m}$. However, the depth of tumor invasion in the U87 Δ EGFR expressing δ -catenin shRNA samples treated with bevacizumab was significantly decreased (mean, $144.9 \pm 60 \mu\text{m}$, $P < 0.05$) (D).

(E) VEGFR-knockdown GBM by shRNA against human VEGFR2 (KDR). a: δ -catenin expression level was not changed by VEGFR2 knockdown. b, c: the number of invasion cells under bevacizumab treatment were decreased when VEGFR2 was knocked down.

(F) According to the IVY glioblastoma atlas project, δ -catenin is highly expressed at the tumor edge and in the infiltrating tumor (© 2017 Allen Institute for Brain Science. Ivy Glioblastoma Atlas Project. Available from: glioblastoma.alleninstitute.org).

Data are shown as the mean \pm SE. Scale bars, 50 μm (A), 200 μm (C), 50 μm (E).

Figure.1

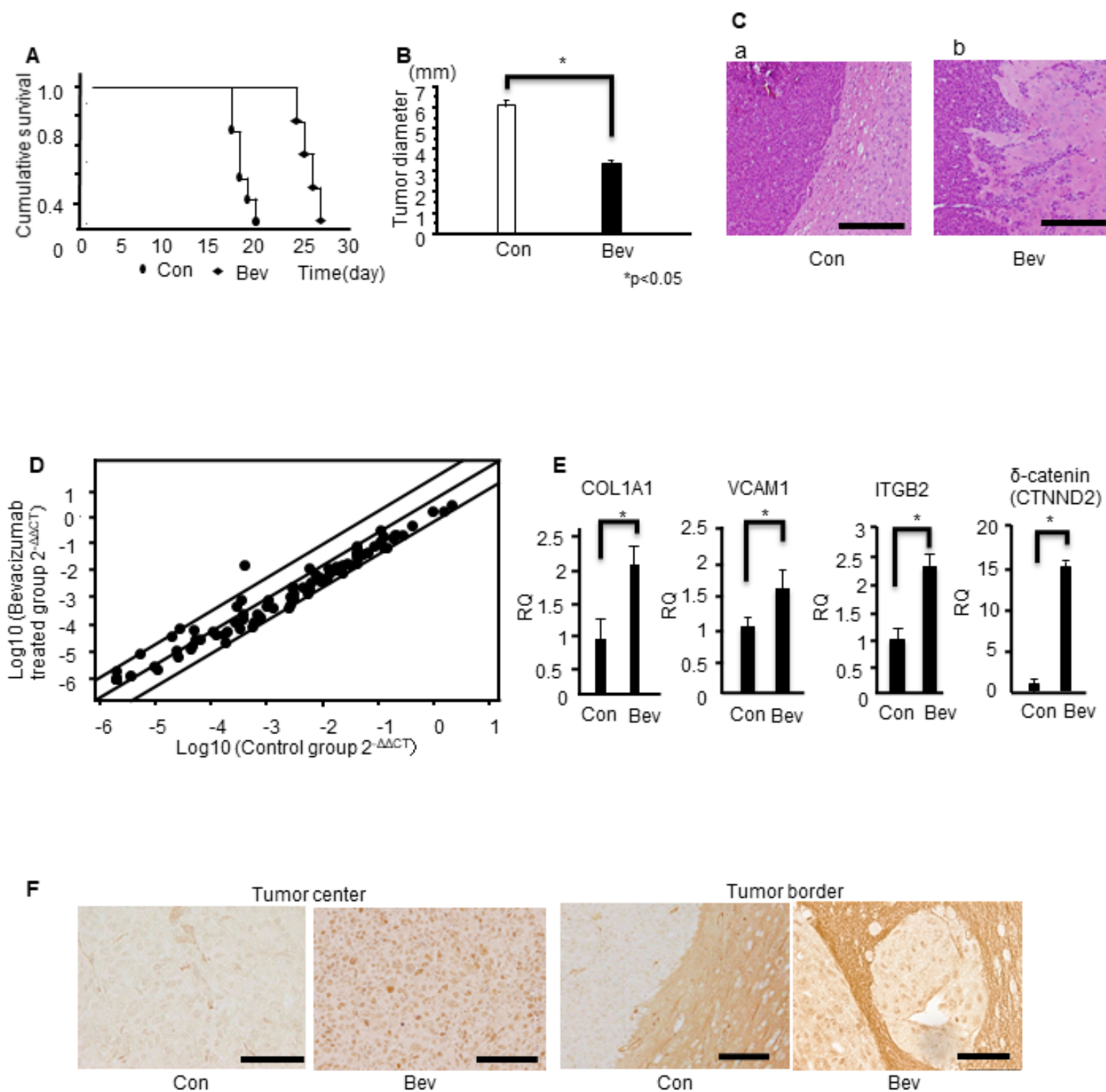


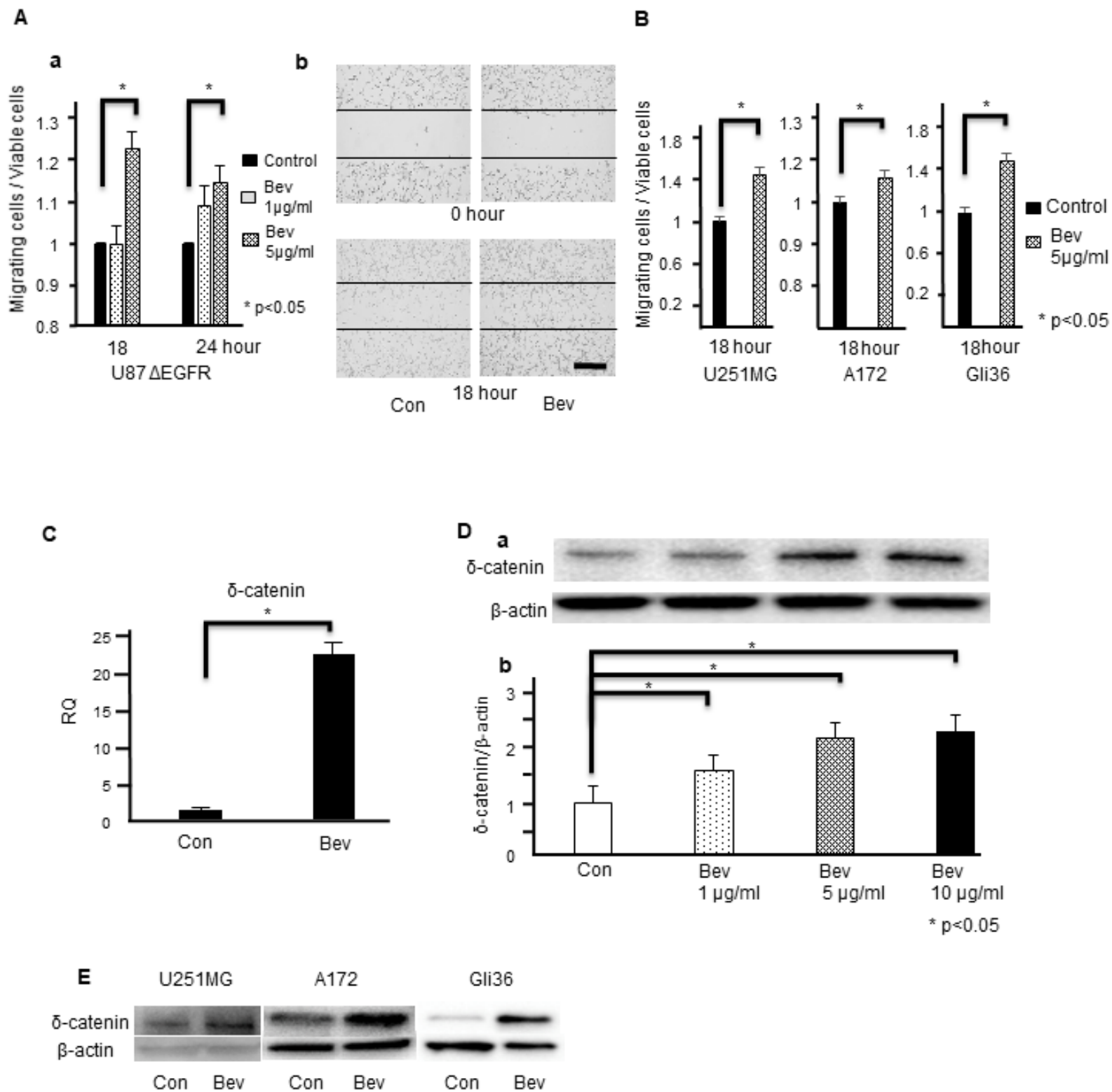
Figure.2

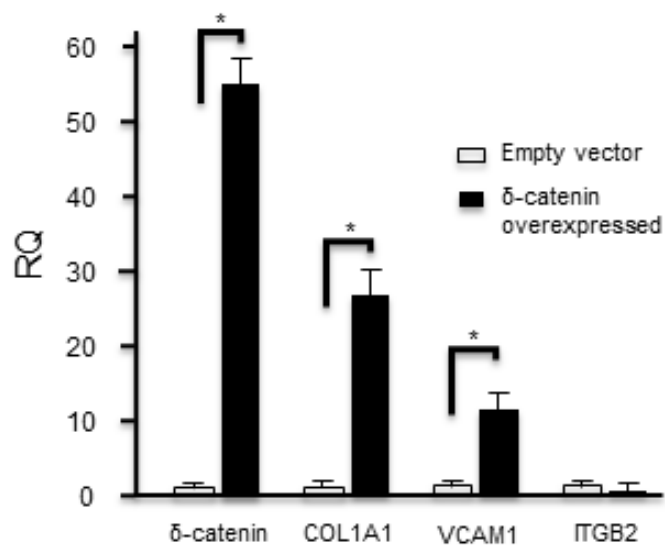
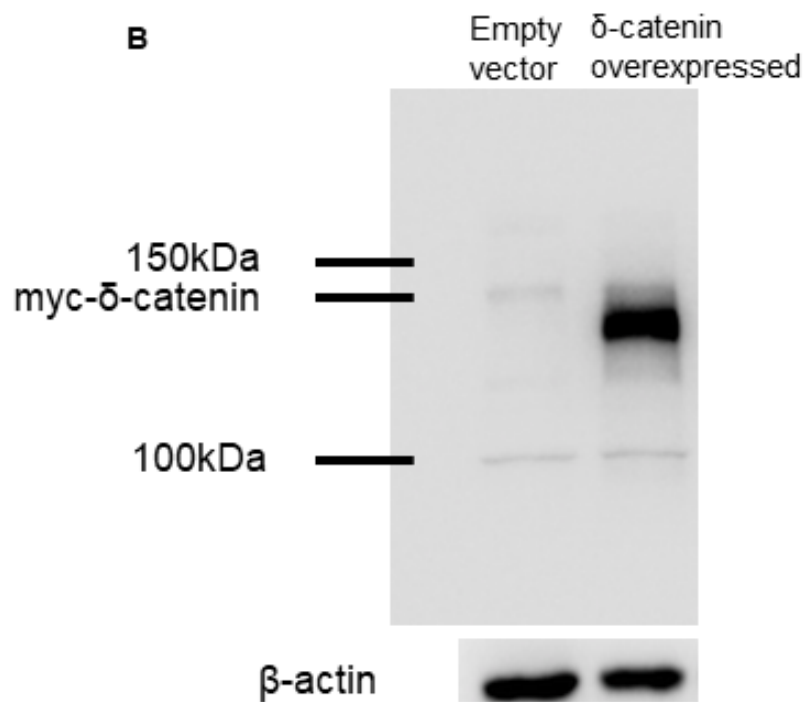
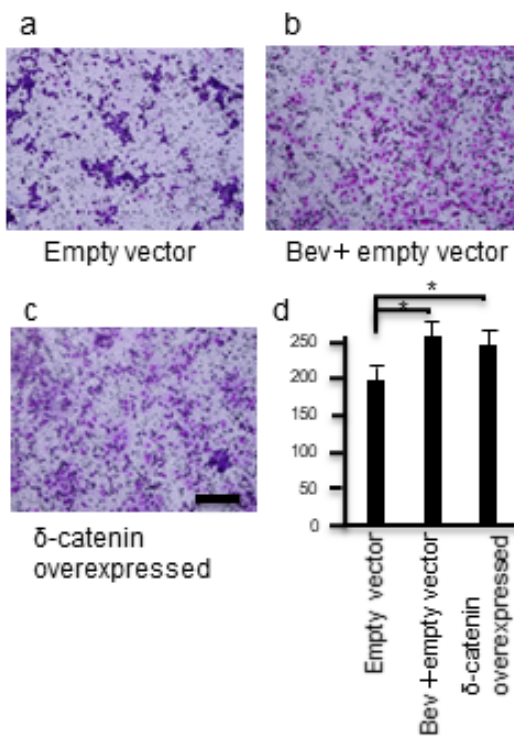
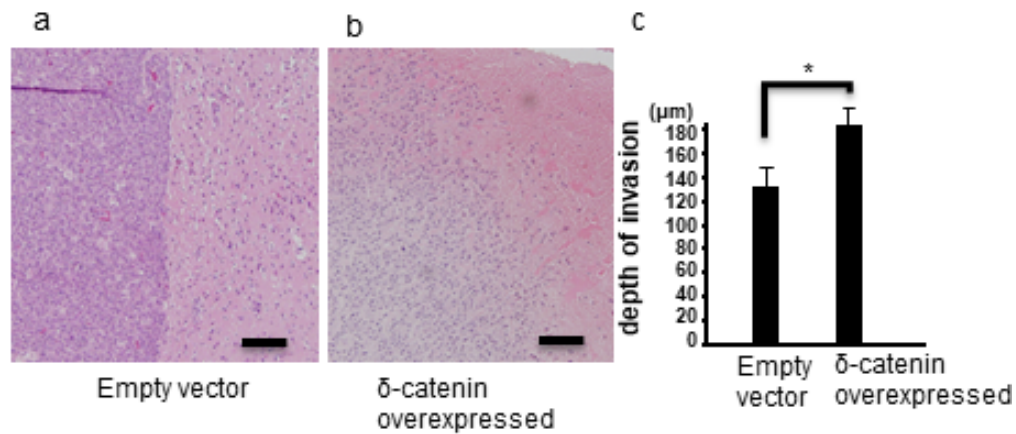
Figure.3**A****B****C****D**

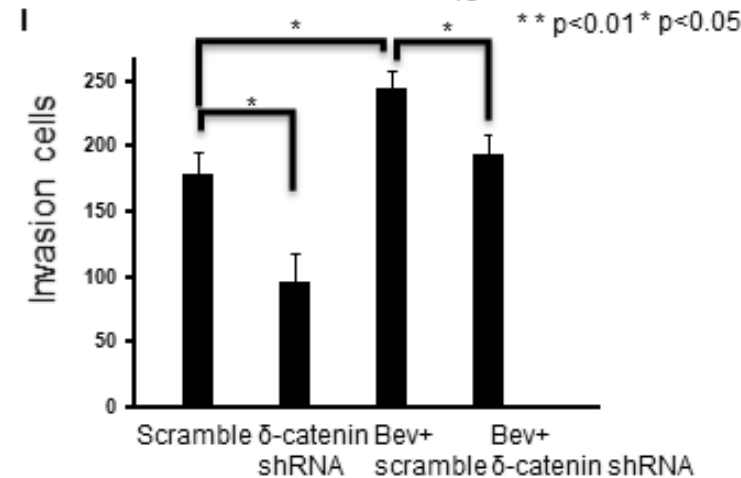
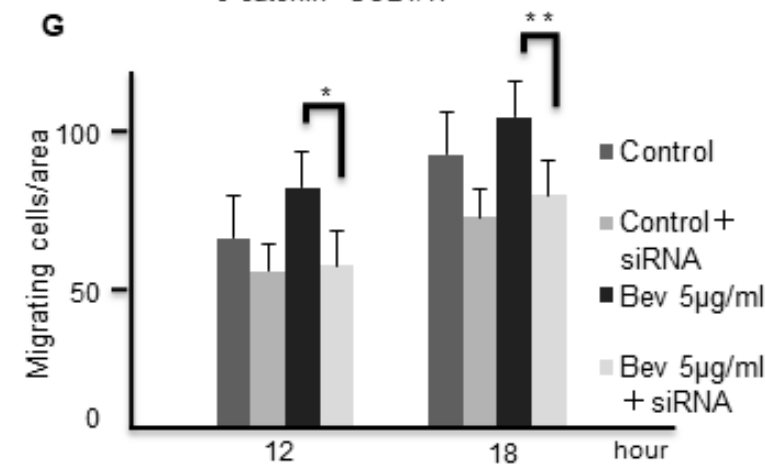
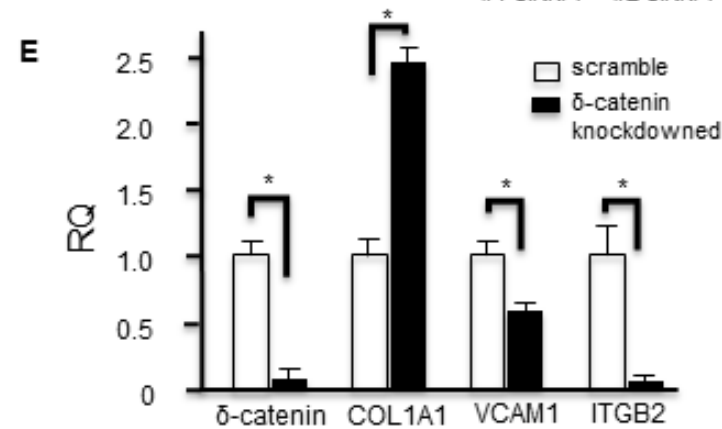
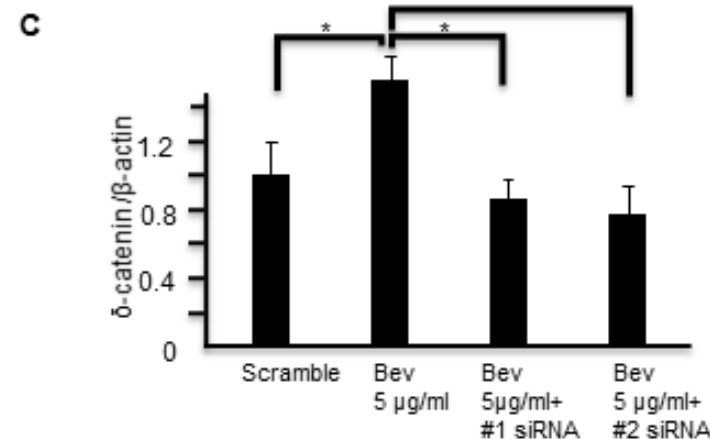
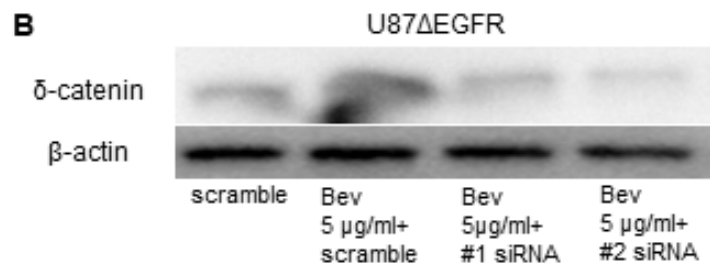
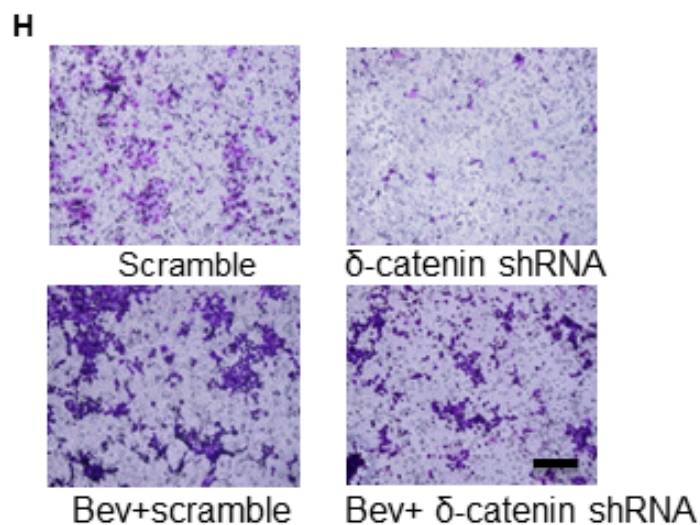
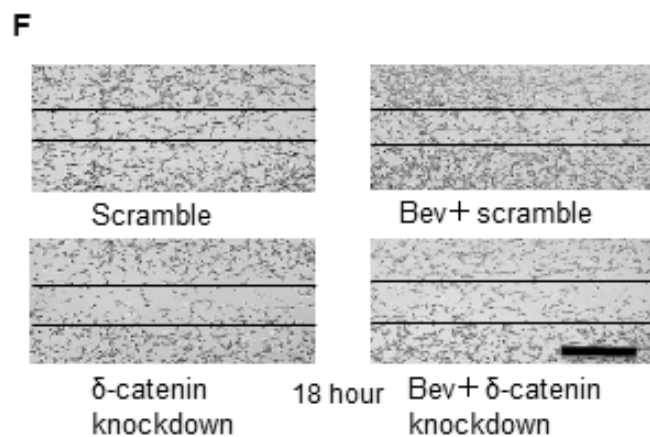
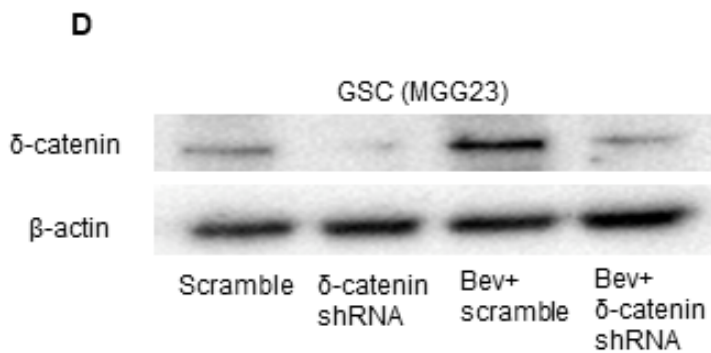
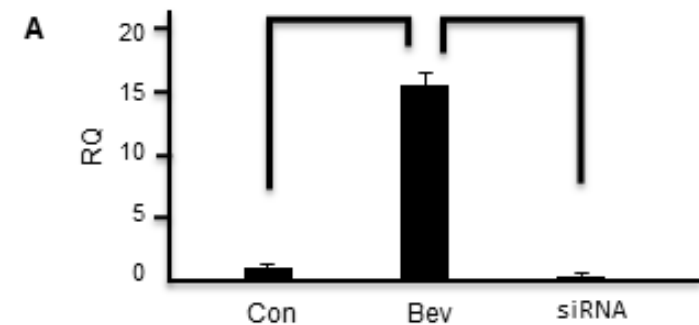
Figure.4

Figure 5